CONTROL AND APPLICATION OF BEAM MICROBUNCHING IN HIGH BRIGHTNESS LINAC-DRIVEN FREE ELECTRON LASERS

G. Stupakov

SLAC National Accelerator Laboratory, Menlo Park, CA, USA

Abstract

We review physical mechanisms and driving forces behind the microbunching instability in modern free-electron lasers. Several methods to fight the instability are presented and evaluated. A recent idea of using the instability for coherent generation of UV radiation is described. Noise suppression in relativistic beams is briefly reviewed.

INTRODUCTION

Modern free-electron lasers are playing an important role in development of new experimental techniques for studies of fundamental properties of matter in chemistry, biology, life sciences, complex materials, etc. Important parts of these FELs are high-brightness, high-current, relativistic electron beams which are typically generated in RF photo guns and compressed longitudinally in magnetic bunch compressors located at several locations in the linac. When such a beam is sent though an undulator, an FEL instability develops driven by the electromagnetic interaction and leading to the longitudinal bunching in the beam at the undulator radiation wavelength. In optimal conditions, this induced bunching results in coherent undulator radiation which can be many orders more intense than the radiation of an un-bunched beam at the entrance to the undulator.

It turns out that transporting high-brightness electron beams through hundreds of meters of the accelerator and compressing it may lead to deterioration of its properties through a mechanism similar to the FEL instability but at much longer wavelengths. It is called the microbunching instability (MBI) and was first demonstrated in computer simulations in Ref. [1]. The existence of this instability is now well established in several FEL-driven accelerators (see, e.g., [2–4]). This instability creates both the energy and density modulations in the beam increasing the energy spread up to the level that can degrade the FEL gain process. An accompanying and undesired effect is a large coherent optical transition radiation signal at intercepting diagnostic screens, often limiting the utility of beam profile imaging systems [5,6].

In this paper we review the mechanism of the instability and various approaches to control it in modern FELs. More details on this subject can be found in the recent publication [7].

SHOT NOISE IN A QUIET BEAM

Before addressing the issue of beam instabilities it is important to understand statistical properties of a "quiet" beam—which is not subjected to such instabilities. In the absence of instabilities it is usually assumed that particles are randomly distributed in space without correlations between their positions[1]. Statistical properties of such a distribution are referred to as *shot noise*. While there are several techniques to describe shot noise, the most general one uses the language of the distribution functions and the formalism of the Vlasov equation. Below we will briefly characterize the distribution function of the shot noise.

We consider fluctuations in the beam in the laboratory frame of reference. The coordinate z marks the position of a particle inside the beam (with positive z in the direction of propagation), and $\eta = \Delta E/E_0$ is the relative energy deviation with the nominal energy of the beam $E_0 = \gamma mc^2$. The 1D distribution function is $f_0(z, \eta) = n_0 F(\eta) + \delta f(z, \eta)$ where $F(\eta)$ is the averaged distribution function normalized by $\int d\eta F(\eta) = 1$, and n_0 is the averaged line density of the beam. Note that we assume on average uniform distribution over z which is a reasonable local approximation for small-scale fluctuations. The fluctuational part $\delta f(z, \eta)$ can be Fourier expanded, $\delta \hat{f}_k(\eta) = \int_{-\infty}^{\infty} dz e^{-ikz} \delta f(z, \eta)$. For shot noise, according to the statistical physics of ideal gas [8],

$$\langle \delta f(z,\eta)\delta f(z',\eta')\rangle = n_0 F(\eta)\delta(z-z')\delta(\eta-\eta'), \quad (1)$$

which after the Fourier transformation gives

$$\langle \delta \hat{f}_k(\eta)\delta \hat{f}_{k'}(\eta')\rangle = 2\pi n_0 F(\eta)\delta(k+k')\delta(\eta-\eta'), \quad (2)$$

where the angular brackets denote ensemble averaging. Introducing the density fluctuation $\delta n(z) = \int d\eta\,\delta f(z,\eta)$ we find by integrating (1) over η and η'

$$\langle \delta n(z)\delta n(z')\rangle = n_0\delta(z-z'). \quad (3)$$

This is a mathematical expression of the properties of the shot noise: density fluctuations in shot noise are uncorrelated in space.

SOURCES OF IMPEDANCE

According to the modern understanding there are two important sources of impedance that drive MBI. The first one is the longitudinal space charge (LSC) impedance (see, e.g., [9]). When a beam of small radius a propagates inside a round pipe of radius r_w with perfectly conducting walls it generates the longitudinal wakefield due to its space charge.

---

[1] More precisely, this is only true when one neglects the Coulomb interaction between the particles which establishes such correlations. This interaction however is typically small in relativistic beams. Correlations can also be imprinted on the beam in the process of electron emission in photo guns.

Assuming $a \ll r_w$, the space charge impedance is given by the following expressions: for $k \equiv \omega/c \ll \gamma/r_w$,

$$Z_{\text{LSC}}(k) \approx i\frac{Z_0 c}{4\pi}\frac{k}{\gamma^2}\left(1 + 2\ln\frac{r_w}{a}\right), \qquad (4)$$

and for $\gamma/a \gg k \gg \gamma/r_w$,

$$Z_{\text{LSC}} \approx i\frac{Z_0 c}{4\pi}\frac{k}{\gamma^2}\left(1 + 2\ln\frac{\gamma}{ak}\right). \qquad (5)$$

At even shorter wavelengths, for $k \gg \gamma/a$, the concept of impedance, strictly speaking, breaks down, because it is only valid if the induced field does not change much through the beam cross section. For analysis of the space charge forces at these short distances see [10, 11]. As a numerical illustration of the region of applicability of Eq. (5) consider the following example: for $a = 100\,\mu m$, $\gamma = 500$, the condition $k \lesssim \gamma/a$ is satisfied for $\lambda = 2\pi/k \gtrsim 1\,\mu m$.

Another driver of the microbunching instability is the so called coherent synchrotron radiation (CSR) impedance. It arises when a relativistic particle is moving in free space in a circular orbit. The CSR wake is localized in front of the particle, $z > 0$. Assuming the orbit radius R and neglecting transition effects the CSR wake of a point charge per unit length of path for the distances $R \gg z \gg R/\gamma^3$ is given by the following equation[2] [12, 13]:

$$w(z) \approx -\frac{E_\parallel}{e} = -\frac{2}{3^{4/3}R^{2/3}z^{4/3}}, \qquad (6)$$

with the corresponding longitudinal CSR impedance

$$Z_{\text{CSR}}(k) = \frac{Z_0}{4\pi}\frac{2}{3^{1/3}}\Gamma\left(\frac{2}{3}\right)e^{i\pi/6}\frac{k^{1/3}}{R^{2/3}}, \qquad (7)$$

where Γ is the gamma-function. These formulas can be used if the transverse beam size $\sigma_\perp$ is not very large, $\sigma_\perp \ll (\lambda^2 R)^{1/3}$ (here $\lambda = 1/k$). Also the transient effects at the entrance to and exit from the magnet can be neglected it $l_{\text{magnet}} \gtrsim (\lambda R^2)^{1/3}$.

1D MODEL OF MICROWAVE INSTABILITY

It is easy to understand the mechanism of MBI if one first recalls a more familiar 1D model of microwave instability in rings. Assuming the wavelength of the instability much smaller than the bunch length, we can consider a coasting beam with current I_0. We also neglect the energy spread in the beam which makes it a cold-beam model. An important element of the instability is the slippage effect: particles with different energy move relative to each other in the longitudinal direction. Consider a small sinusoidal perturbation on the beam, with the linear beam density $n(z,t) = n_0 + n_1(z,t)$, where $n_1 \ll n_0$ ($n_0 = I_0/ec$ for relativistic beams, with I_0 the beam current).

---

[2] An apparent divergence of the wake (6) is removed in calculation of the bunch wake through integration by parts.

The microwave instability is described by the following equations. The linearized continuity equation

$$\frac{\partial n_1}{\partial t} + n_0\frac{\partial v_{\text{sl}}}{\partial z} = 0 \qquad (8)$$

involves the slippage "velocity" v_{sl} that is proportional to the relative energy deviation $\eta = \Delta E/E_0$ and the slippage factor ν,

$$v_{\text{sl}}(z,t) = -c\nu\eta(z,t). \qquad (9)$$

The energy deviation is caused by the wakefield,

$$\frac{\partial \Delta E(z,t)}{\partial t} = -ce^2\int w(z'-z)n_1(z',t)dz'. \qquad (10)$$

Assuming all the perturbations $\propto e^{-i\omega t + ikz}$ and introducing the impedance instead of the wake, $Z(k) = c^{-1}\int w(z)e^{ikz}dz$, we arrive at the following dispersion relation:

$$\omega^2 = i\frac{c^3 r_e n_0 k\eta}{\gamma}Z(k). \qquad (11)$$

The imaginary part $\Gamma = \text{Im}\,\omega$ gives the growth rate of the instability. We see that almost any impedance will cause an instability if Z is complex (only for purely inductive impedance $Z = -i\omega L$, with L the inductance, the beam is stable). The growth rate scales as $\Gamma \propto \sqrt{I_0}$.

The mechanism of this instability can be explained as a sequence of the following cycles. An initial current perturbation I_1 in the beam induces an energy modulation $\Delta E = eZI_1$ by the impedance. The slippage translates ΔE into the density perturbation Δn and hence to I_2. Under certain conditions, the final perturbation I_2 is greater than I_1 and keeps growing with each cycle.

MBI IN BUNCH COMPRESSOR

The theory of MBI in bunch compressors was developed in 2001-2002 in Refs. [14–17]. The physics of the instability is similar to the microwave instability considered in the previous section, however, it uses a different language to characterize the instability.

Again, we consider a longitudinally uniform beam with an initial density modulation given by $n(z) = n_0 + n_i \sin k_i z$ with $\lambda_i = 2\pi/k_i$ the wavelength of the initial perturbation. The beam is sent through a chicane shown in Fig. 1. The
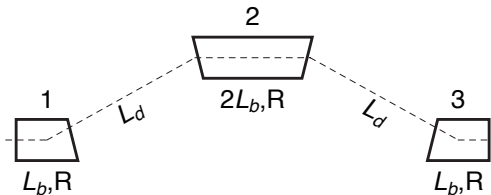

Figure 1: A model of magnetic chicane consisting of three magnets with the middle one two times longer than the first and the last ones. The magnet lengths are L_b, $2L_b$ and L_b, the bending radius in the magnets is R, and the distance between the magnets is L_d.

05 Beam Dynamics and Electromagnetic Fields

D05 Instabilities - Processes, Impedances, Countermeasures

beam has an energy chirp, and after the passage through the chicane the density becomes $n(z) = n_0 + n_f \sin k_f z$ where the final wavenumber is larger than the initial one due to the compression, $k_f = Ck_i$, with C the compression factor. If there is an instability, the final beam density is amplified with the amplification factor, or gain, defined as

$$G(k_i) = \frac{n_f}{n_i}. \tag{12}$$

A relatively simple model for the calculation of the gain factor G was proposed in [16]. The model assumes the CSR wake in the magnets as a driving force of the instability and a cold beam. Take an initial current perturbation $I = I_0 + I_1 \cos kz$ with $I_1 \ll I_0$. After passage through the first magnet the energy modulation in the beam is $\Delta E = eV = eL_b Z_{CSR}(ck)I_1$. Propagation from magnet 1 to 2 shifts the particles by $\Delta z = (\Delta E/E)R_{56}^{(1\to2)}$, where $R_{56}^{(1\to2)}$ is the R_{56} element of the transport matrix R from magnet 1 to 2. It follows from the continuity equation (8) that the slippage induces density and hence current perturbations, $I_2 = k\Delta z I_0$. Assuming $I_2 \gg I_1$ we can neglect I_1. After passage through magnet 2 the energy modulation is $\Delta E = eV = 2L_b e Z_{CSR}(ck)I_2$. Propagation from magnet 2 to 3 shifts the particles by $\Delta z = (\Delta E/E)R_{56}^{(2\to3)}$, which induces the density perturbation $I_3 = k\Delta z I_0$. Again assuming $I_3 \gg I_2$ we neglect I_2 and obtain the gain factor $G = I_3/I_1$ [16]:

$$G = \frac{2\Gamma^2(2/3)}{3^{5/3}} \frac{I_0}{\gamma I_A} \frac{k^{8/3}|R_{56}|^2 L_d^2}{R^{4/3}}, \tag{13}$$

where Γ is the gamma-function, $I_A = m_e c^3/e = 17$ kA, and R_{56} is the dispersive strength of the whole chicane. Note a strong dependence of G versus the wavenumber k.

More sophisticated models of MBI involve a solution of the Vlasov equation for the evolution of the distribution function through the system. They take into account the energy spread of the beam σ_E, its finite emittance ϵ, and the compression effect due to the energy chirp. They predict that σ_E and ϵ tend to suppress the gain G through the mechanism that is often associated with Landau damping, but in reality is a simple smearing of the induced perturbations due to the variable slippage of particle with different energies, see Fig. 2. The smearing of microbunching due to the energy
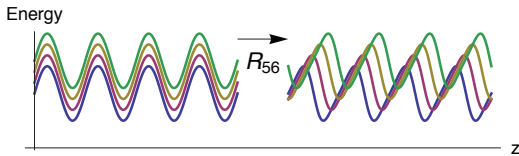
Energy

Figure 2: Illustration of the smearing effect of the energy spread. Different colors show perturbations of particle with different energies. Due to the slippage dependence versus energy and initially phased waves de-phase when they propagate through the system.

spread is effective if

$$R_{56}\frac{\sigma_E}{E} \gtrsim \lambda. \tag{14}$$

In more accurate calculations the following factor should be added to the gain (13)

$$e^{-C^2k^2(\sigma_E/E)^2R_{56}^2/2} \times e^{-C^2k^2(\epsilon/2\beta)(\beta^2R_{51}^2+R_{52}^2)}, \tag{15}$$

where β is the beta function in the chicane, C is the compression factor and R_{51} and R_{52} are the corresponding transport matrix elements for the chicane.

The exponential suppression of the large values of k in (15) counteracts the fast growth of G in (13) and leads to a typical profile of G which has a maximum at intermediate wavelengths. As an example, Fig. 3 shows the MBI gain calculated for LCLS for two scenarios: with the initial $\sigma_E \sim 3$ keV, and with an increased energy spread achieved through a strong superconducting wiggler added to the system after the first bunch compressor.
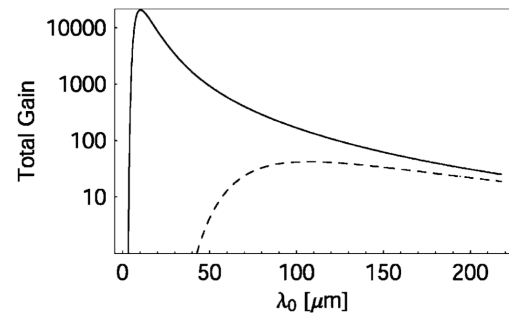

Figure 3: MBI gain calculated for LCLS as a function of the initial modulation wavelength λ_0 with $\sigma_E \sim 3$ keV (solid curve) and the energy spread increased by about a factor of 10 (dashed curve) (from Ref. [18]).

USING LASER HEATER TO SUPPRESS MBI

As is outlined in the previous section, a beam with a larger energy spread is less susceptible to the instability. An effective method to "heat up" the beam by increasing its uncorrelated energy spread through a laser-beam interaction in an undulator was proposed in Ref. [19] and was later given the name of a "laser heater". The required slice energy spread of the beam is set to the level which, on the one hand, suppresses development of the microbunching instability, but, at the same time, is small enough to not impede lasing in the FEL. The laser heater works by introducing a correlated microstructure in the phase space of the beam on the scale of the laser wavelength that is effectively washed out through transport, resulting in an increase of the uncorrelated energy spread. Laser heater is now considered as a necessary attribute in practically all designs of modern x-ray FELs [20–22].

In a laser heater a laser-beam of power P_L and waist w_0 interacting with electrons in an undulator of length L_u modulates the beam energy $\Delta E = m_e c^2 \Delta\gamma(r)\cos(k_L z + \phi)$ with

$$\Delta\gamma(r) = \sqrt{\frac{P_L}{P_0}} \frac{2KL_u}{\gamma w_0} \mathcal{J} e^{-r^2/w_0^2}, \tag{16}$$

where r is the radial position, $k_L = 2\pi/\lambda_L$ with λ_L the laser wavelength, $P_0 = I_A m_e c^2/e \approx 8.7$ GW, K is the undulator parameter, and the factor e^{-r^2/w_0^2} describes the radial profile of the laser beam. To find the resulting energy distribution of the electron beam this formula should be combined with the transverse beam distribution (see details in [18]). Depending on the ratio of the rms transverse beam size σ_x ($\sigma_x \approx \sigma_y$) and the laser beam size $\sigma_r = w_0/2$, one finds either a double-horn energy distribution (in the limit $\sigma_r \gg \sigma_x$) or a Gaussian-like distribution (when the laser pulse is matched to the beam size, $\sigma_x \approx \sigma_r$).

The first laser heater was included into the design of LCLS. Experimental results obtained on the LCLS heater are documented in Ref. [23]. Fig. 4 shows the longitudinal phase space of the beam measured with the help of an rf deflecting cavity. The figure clearly shows the increase of the beam
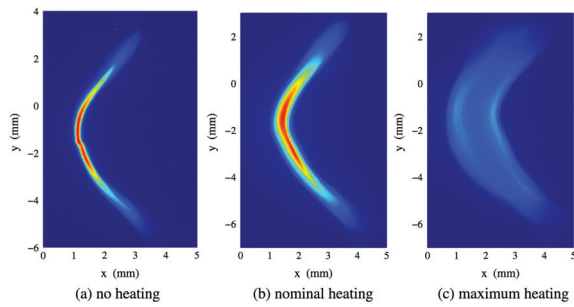

Figure 4: Measured longitudinal phase space at 135 MeV with (a) laser heater off, (b) IR-laser energy at 10 μJ, and (c) at 220 μJ. The vertical axis shows beam longitudinal position and the horizonal axis shows the beam energy (from Ref. [23]).

energy spread with the energy of the laser pulse.

In a recent paper from FERMI FEL [24] the authors studied regimes when the laser heater produces a non-Gaussian distribution function. They showed that such a distribution can provide additional advantages in a subsequent HGHG seeding used at FERMI for generation of high harmonics of the seeding laser.

SUPPRESSION OF MBI WITHOUT LASER HEATER

Several new methods of fighting the MBI where studied in recent years [25–29].

The authors of [25] proposed to suppress the instability by introducing a strong chicane located close to the end of the accelerator which would smear out the energy modulation accumulated in the beam in an upstream sections of the accelerator (see the first term in (15)). It is important that at the entrance to this strong chicane the energy chirp is removed, otherwise a strong undesired compression would ensue. An experimental demonstration of the method is reported in Ref. [26].

In a different approach, a reversible heater is proposed in [27] using two transverse deflecting cavities (TDS), be-

fore and after the bunch compressor, in combination with a special lattice between them. Both TDS are set up at zero-crossing rf phase. The first transverse cavity, in addition to the varying with time transverse deflection, induces a transversely correlated energy spread in each slice of the beam, related to the principle of TDS through Panofsy-Wenzel theorem. When the beam with increased energy spread passes through the chicane the increased longitudinal slippage destroys the energy modulation in the beam effectively suppressing MBI. The energy spread is then removed by the second deflecting cavity located after the chicane. Detailed simulations show effectiveness of the proposed system, although it imposes challenging requirements on the energy jitter of the beam and rf phase jitter in TDS.

USING MBI FOR GENERATION OF UV RADIATION

While MBI poses a danger to the FEL perfomance and various ways are employed to suppress it, an interesting idea of intentionally submitting the beam to a small-scale MBI for generation of vacuum ultraviolet and x-ray radiation in FELs was proposed in Ref. [30]. The setup of an LSC amplifier
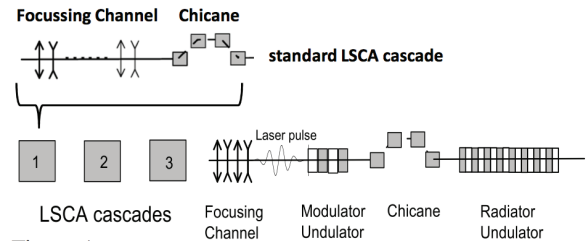

Figure 5: Standard LSCA cascade and LSCA-based attosecond scheme (from Ref. [31]).

consists of a sequence of focusing channels and chicanes shown in Fig. 5. The focusing strength of the channels and the dispersive properties of the chicanes are optimized so as to increase the gain G of the system for a given wavelength λ. An example of an optimized setup is considered in [30] for the following beam parameters: the electron beam energy 3 GeV, peak current 2 kA, normalized emittance 2 μm, and rms energy spread 0.3 MeV. With the beta function $\beta = 1.4$ m and $R_{56} = 25$ μm one can achieve the total gain of about $G = 10^3$ at the wavelength $\lambda \approx 15$ nm. The length of the drift space is about 20 m. After the last chicane a tunable-gap undulator with the period length of 5 cm and a number of periods 30 is installed. The undulator selects a relatively narrow band of about 3% from the broadband density modulations. The peak power within the central cone is estimated at a gigawatt level.

In a further development of this idea [31] the authors utilize the broadband nature of the MBI amplification and show how one can achive attosecond pulses of radiation in this scheme.

05 Beam Dynamics and Electromagnetic Fields

D05 Instabilities - Processes, Impedances, Countermeasures

NOISE SUPPRESSION

While MBI starting from shot noise increases the density fluctuation in the beam, the same interaction between the particles, under proper conditions, can lead to noise suppression. The interest to noise suppression at short wavelengths in motivated, to large part, by requirements of FEL seeding. Suppressing the initial noise in the beam, one would require less power in the seeding system. In the last few years, several groups have independently proposed suppressing shot noise at short wavelengths in relativistic electron beams [32–35].

A simple setup for noise suppression is shown in Fig. 6. A beam with shot noise is injected into an interaction region of length L, followed a dispersion region with a proper value of R_{56}. Calculations show that the noise is suppressed if the

Figure 6: Schematic of a noise suppression system.

following condition is satisfied [35]

$$\frac{4\pi e^2 L}{S E_0} n_0 R_{56} = 1, \qquad (17)$$

where L is the length of the interaction region, S is the beam area, E_0 is the beam area, n_0 is the number of particle per unit length and R_{56} is the dispersive strength of the chicane.

First experimental observations of shot noise suppression at sub-micron wavelengths were recently reported in [36, 37].

CONCLUSIONS

The design of modern FEL is influenced and constrained by the need to preserve the properties of high-brightness, high-current electron beam in the process of acceleration and transportation through the system where the beam is subjected to MBI. In this paper we reviewed the physical mechanisms and driving forces behind the instability. We presented the laser heater idea as an accepted method of fighting MBI and also gave a review of various new ideas to suppress MBI. Noise suppression in the relativistic beams was discussed as another method of controlling microbunching in relativistic beams.

REFERENCES

[1] M. Borland, *et al.*, NIM **A483**, 268 (2002).

[2] T. Shaftan and Z. Huang, PRST-AB **7**, 080702 (2004).

[3] R. Akre, *et al.*, PRST-AB **11**, 030703 (2008).

[4] A. H. Lumpkin, R. J. Dejus, and N. S. Sereno, PRST-AB **12**, 040704 (2009).

[5] H. Loos, *et al.*, in *Proc. of the 2008 FEL Conference, paper THBAU01*, Gyeongju, Korea (2008).

[6] C. Behrens, *et al.*, PRST-AB **15**, 062801 (2012).

[7] S. Di Mitri and M. Cornacchia, Physics Reports, in press, (2014).

[8] E. M. Lifshitz and L. P. Pitaevskii, *Physical Kinetics*, (Pergamon, London, 1981).

[9] S. Y. Lee, *Accelerator Physics* (World Scientific, 1999).

[10] M. Venturini, PRST-AB **11**, 034401 (2008).

[11] A. Marinelli and J. B. Rosenzweig, PRST-AB **13**, 110703 (2010).

[12] Y. S. Derbenev *et al.*, DESY FEL Report TESLA-FEL 95-05, Hamburg, Germany (1995).

[13] J. B. Murphy, S. Krinsky, and R. L. Gluckstern, in *Proc. IEEE PAC, Dallas, 1995* (IEEE, Piscataway, NJ, 1996).

[14] M. Borland, PRST-AB **4**, 070701 (2001).

[15] S. Heifets, G. Stupakov, and S. Krinsky, PRST-AB **5**, 064401 (2002).

[16] E. L. Saldin, E. A. Schneidmiller, and M. V. Yurkov, NIM **A490**, 1 (2002).

[17] Z. Huang and K.-J. Kim, PRST-AB **5**, 074401 (2002).

[18] Z. Huang, *et al.*, PRST-AB **7**, 074401 (2004).

[19] E. Saldin, E. Schneidmiller, and M. Yurkov, NIM **A528**(1-2), 355 (2004).

[20] J.-H. Han, H.-S. Kang, and I. S. Ko, in *Proc. of the 2012 IPAC* (2012), p. 1735.

[21] S. Spampinati, *et al.*, in *Proc. of the FEL Conference 2012* (2012), p. 177.

[22] G. Angelova, *et al.*, in *2008 European PAC* (2008), p. 2695.

[23] Z. Huang, *et al.*, PRST-AB **13**, 020703 (2010).

[24] E. Ferrari, *et al.*, PRL **112**, 114802 (2014).

[25] S. Di Mitri, *et al.*, PRST-AB **13**, 010702 (2010).

[26] S. Di Mitri and S. Spampinati, PRL **112**, 134802 (2014).

[27] C. Behrens, Z. Huang, and D. Xiang, PRST-AB **15**, 022802 (2012).

[28] J. Qiang, C. E. Mitchell, and M. Venturini, PRL **111**, 054801 (2013).

[29] D. Douglas, *et al.*, Tech. Rep. JLAB-ACP-14-1751 (2014).

[30] E. A. Schneidmiller and M. V. Yurkov, PRST-AB **13**, 110701 (2010).

[31] M. Dohlus, E. Schneidmiller, and M. Yurkov, in *Proc. of the 2nd IPAC*, San Sebastián, Spain (2011), p. 1449.

[32] A. Gover and E. Dyunin, PRL **102**, 154801 (2009).

[33] A. Nause, E. Dyunin, and A. Gover, J. of Appl. Phys. **107**(10), 103101 (2010).

[34] V. N. Litvinenko, in *Proc. of the 2009 FEL Conf.*, Liverpool, UK (2009), p. 229.

[35] D. Ratner, Z. Huang, and G. Stupakov, PRST-AB **14**, 060710 (2011).

[36] D. Ratner and G. Stupakov, PRL **109**, 034801 (2012).

[37] A. Gover, *et al.*, Nat. Phys. **8** (12), 877 (2012).